

Supporting Information

A neutral crystalline imino-substituted silyl radical

Fiona J. Kiefer,^a Arseni Kostenko,^a Richard Holzner,^a Shigeyoshi Inoue^{*a}

^aTUM School of Natural Sciences, Department of Chemistry, Wacker-Institute of Silicon Chemistry and Catalysis Research Center, Technische Universität München, Lichtenbergstraße 4, 85748 Garching bei München, Germany. E-Mail: s.inoue@tum.de

Contents

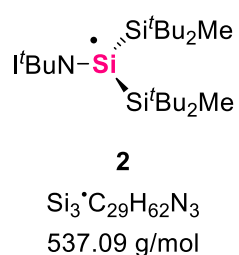
1 Experimental	2
1.1 General Methods and Information	2
1.2 Silyl Radical via disilene reduction	3
1.3 Silyl Radical via Reaction Pathway A.....	6
1.4 Silyl Radical via Reaction Pathway B.....	10
2 Single crystal X-Ray diffraction	13
2.1 General Information.....	13
2.2 SC-XRD Structure	14
2.3 Crystal Data and Structural Refinement Parameters	15
3 Computational Details	17
3.1 General Information.....	17
3.2 Cartesian coordinates and energies of the optimized geometries at the r ² SCAN-3c level	17
4 References.....	19

1 Experimental

1.1 General Methods and Information

All manipulations were carried out under argon atmosphere using standard Schlenk or glovebox techniques and glassware was flame-dried before use. Unless otherwise stated, all chemicals were purchased from Sigma-Aldrich or ABCR and used as received. All solvents were refluxed over sodium/benzophenone, distilled via vacuum transfer, and deoxygenated before use. Deuterated benzene (C_6D_6) was obtained from Sigma-Aldrich and dried over 3 Å molecular sieves. The nuclear magnetic resonance spectra (NMR) were recorded on a Bruker AV500C (1H : 500.36 MHz, ^{29}Si : 99.41 MHz) spectrometer in C_6D_6 at ambient temperature (300 K). The 1H and $^{29}Si\{^1H\}$ NMR spectroscopic chemical shifts δ are reported in ppm relative to tetramethylsilane. 1H and $^{13}C\{^1H\}$ NMR spectra are calibrated against the residual proton and natural abundance carbon resonances of the respective deuterated solvent as internal standard (C_6D_6 : $\delta(^1H) = 7.16$ ppm). All NMR samples were prepared under argon in a *J. Young* PTFE tube. *N*-heterocyclic imin $ItBuN-SiBr_3$ **3** and Imino(silyl)disilene **1** were synthesized according to the literature.¹ Carbon monoxide (CO) 4.7 ($\geq 99.997\%$) was purchased from *Westfalen AG* and used as received. EPR spectra were recorded in a *JEOL JES-FA 200* spectrometer at X-band frequency at room temperature and $T = 163K$. The spectra were measured at a microwave frequency of ca. 9.26 GHz with a microwave power of 5 mW, with modulation amplitude of 0.04 mT sweep time 4 min, sweep width 20 mT, time constant 0.1 s and a modulation frequency of 100 kHz. Simulation of the EPR spectra was performed with the *Easyspin* toolbox for *Matlab*.² Quantitative elemental analyses (EA) were measured with a *EURO EA (HEKAtech)* instrument equipped with a CHNS combustion analyzer at the *Laboratory for Microanalysis* at the *TUM Catalysis Research Center*.

1.2 Silyl Radical via disilene reduction



An impure sample of disilene $t\text{BuN}(t\text{Bu}_2\text{MeSi})\text{Si}=\text{Si}(\text{Si}t\text{Bu}_2\text{Me})\text{N}t\text{Bu}$ (**1**) (100 mg, 132 μmol , 1.00 eq.) was dissolved in toluene (5 mL) and degassed in a pressurizeable Schlenk flask. The mixture was exposed to carbon monoxide (1 bar) at -40°C . Within 30 minutes, the mixture turned orange and slightly cloudy. All volatiles were removed in vacuo, and the residue was extracted with *n*-hexane (3×1 mL). The resulting solution was concentrated under reduced pressure and cooled to -35°C . Compound **2** was obtained as orange crystals (6.00 mg, 11.2 μmol , 8% yield). These crystals were also suitable for SC-XRD analysis.

Note: The reaction was not reproducible with a pure sample of disilene **1**, therefore reaction pathways A and B were explored.

EPR (*n*-hexane, 286 K) $g = 2.0034$

EA:	$\text{Si}_3\text{C}_{29}\text{H}_{62}\text{N}_3$	Calculated [%]:	C (64.85), H (11.64), N (7.82)
		Experimental [%]:	C (62.46), H (11.64), N (7.88)

Note: The carbon value was reproducibly low, presumably due to the formation of incombustible silicon carbides.

Table 1 Details for the EPR measurement of **2**.

Parameters used for the EPR measurement of 2 *	
solvent	<i>n</i> -hexane
<i>T</i> [K]	286
ν [GHz]	9.265
<i>MW</i> [mT]	0.4
<i>TC</i> [s]	0.1
<i>P</i> [mW]	5
<i>RG</i> [dB]	400
<i>CF</i> [mT]	331
<i>SW</i> [mT]	10

**T* = temperature, ν = microwave frequency, *MW* = modulation width, *TC* = time constant, *P* = microwave power, *RG* = receiver gain, *CF* = center field, *SW* = sweep width

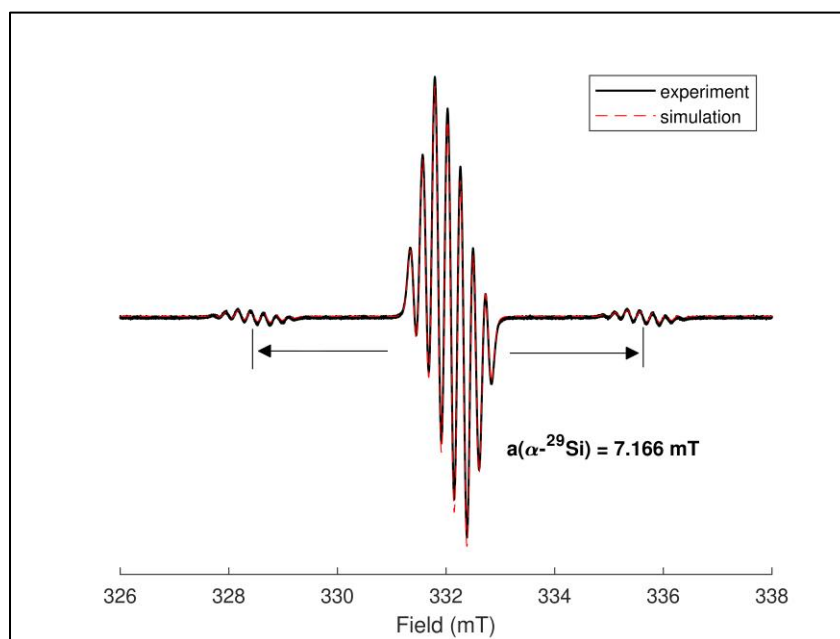


Figure 1 X-band EPR spectrum of **2** in *n*-hexane (2×10^{-3} M) at 286 K; (black) experimental, (red) simulation, overlaid view.

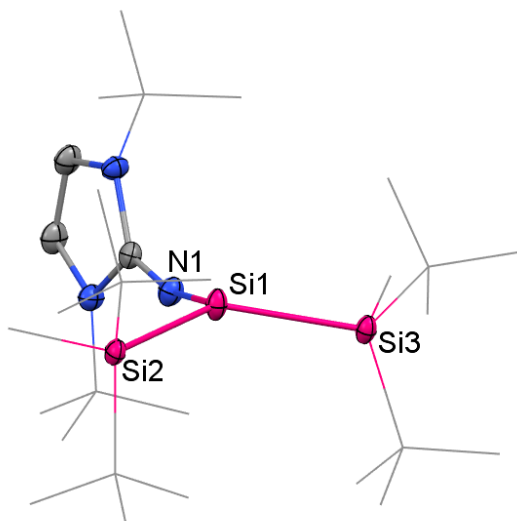
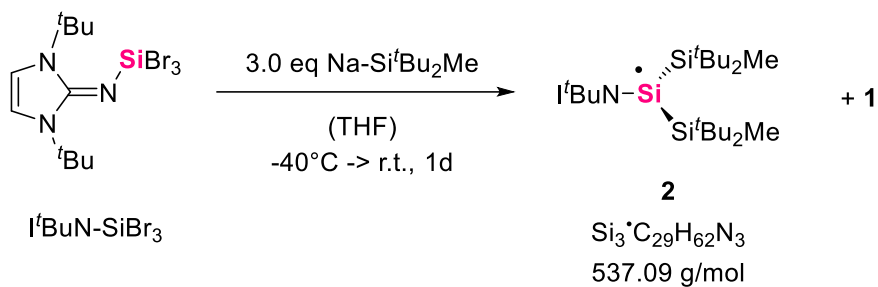


Figure 2 SC-XRD structure of the silyl radical **2**, with thermal ellipsoids drawn at the 50% probability level. Hydrogen atoms are omitted for clarity, ^tBu- and Me-groups are simplified as wireframes. Selected bond lengths [Å] and angles [°]: Si1–Si2 2.3843(7), Si1–Si3 2.3790(8), Si1–N1 1.676(2), N1–C1 1.280(3), Si2–Si1–Si3 132.98(3), Si3–Si1–N1 108.91(7), N1–Si1–Si2 111.62(7).

Note: Compound **2** was obtained with a poor yield, and the synthesis was not perfectly reproducible. Nonetheless, it was fully characterized by EPR spectroscopy, SC XRD analysis, and elemental analysis.

1.3 Silyl Radical via Reaction Pathway A



N-heterocyclic imin $\text{I}^t\text{BuN-SiBr}_3$ (17.1 mg, 36.9 μmol , 1.0 eq.) and silanide $\text{Na-Si}^t\text{Bu}_2\text{Me}$ (20.0 mg, 111 μmol , 3.0 eq.) were mixed, the solids cooled to -40°C , and THF (2 mL) was added. The reaction mixture immediately showed a deep red color. The reaction mixture was warmed to room temperature and stirred for one day. All volatiles were removed in vacuo, and the residue was extracted with *n*-hexane (3×0.5 mL). After drying *in vacuo*, a mixture of **1** and **2** was obtained in moderate yield (19.0 mg, 35.4 μmol , 95% yield). The EPR spectrum (Figure 3) was recorded by filtering 15.0 mg of dissolved reaction mixture in 1 mL *n*-hexane. The unusually high concentration was necessary to observe the splitting of signals. Byproducts Imino(silyl)disilene **1** and disilane $[\text{Me}^t\text{Bu}_2\text{Si}]_2$ could be identified via ^1H and ^{29}Si NMR spectroscopy.

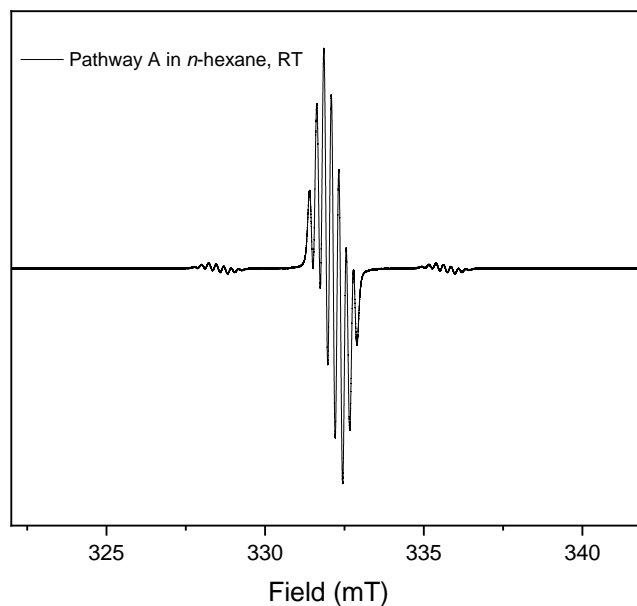


Figure 3: X-band EPR spectrum of **2**, via pathway A in *n*-hexane (2×10^{-1} M) at 286 K; (black) experimental.

Table 2 Details for the EPR measurement of **2**,
Pathway A.

Parameters used for the EPR measurement of 2 *	
solvent	<i>n</i> -hexane
<i>T</i> [K]	286
ν [GHz]	9.265
<i>MW</i> [mT]	0.4
<i>TC</i> [s]	0.1
<i>P</i> [mW]	5
<i>RG</i> [dB]	400
<i>CF</i> [mT]	331
<i>SW</i> [mT]	20

**T* = temperature, ν = microwave frequency, *MW* = modulation width, *TC* = time constant, *P* = microwave power, *RG* = receiver gain, *CF* = center field, *SW* = sweep width

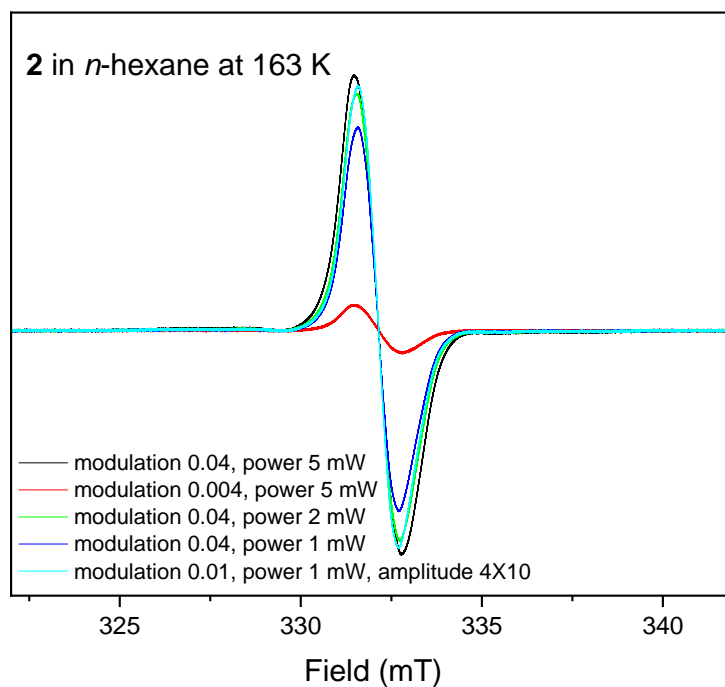


Figure 4 Frozen-solution X-band EPR spectrum of **2**, via pathway A in *n*-hexane (2×10^{-1} M) at 163 K, with various modulations.

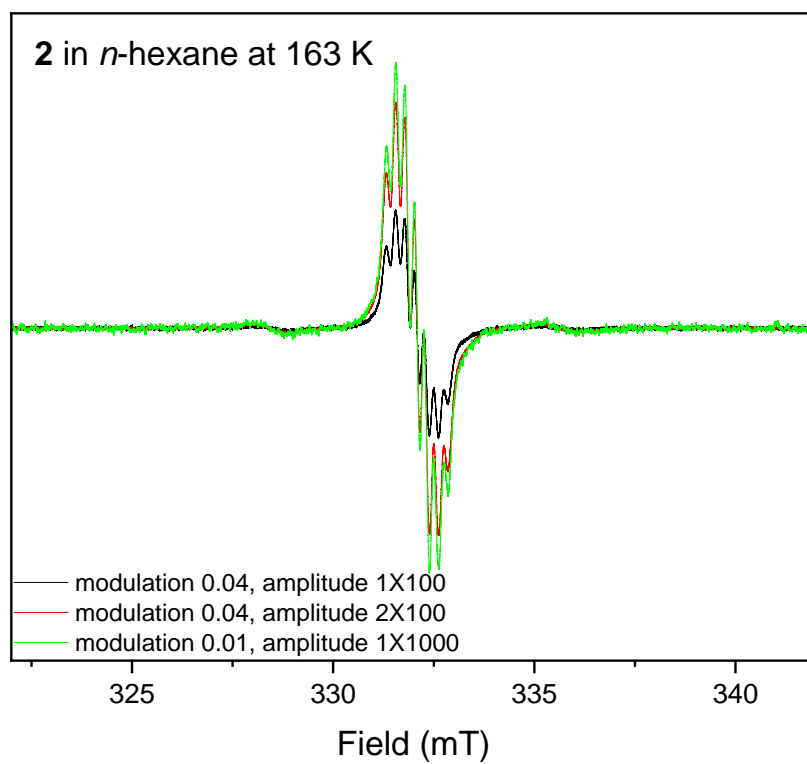


Figure 5 Frozen-solution X-band EPR spectrum of **2**, via pathway A in *n*-hexane (2×10^{-3} M) at 163 K, with various modulations.

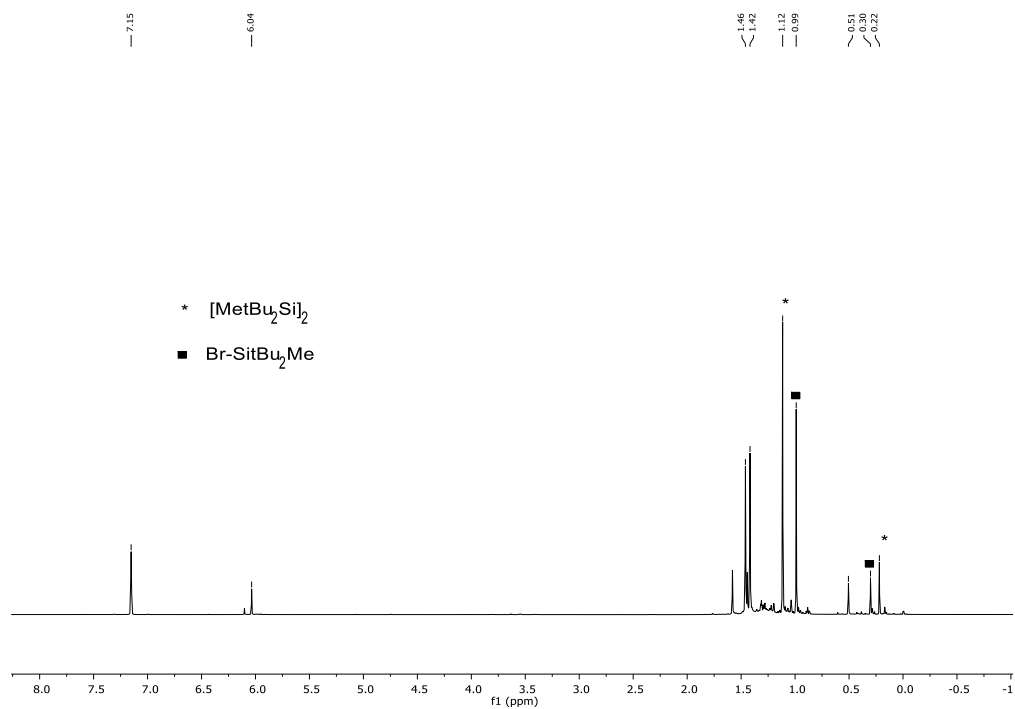


Figure 6 ^1H NMR spectrum of **2**, via Pathway A. Disilene **1** δ [ppm]: 6.11, 6.04, 1.47, 1.42, 0.51. Disilane $[\text{Me}'\text{Bu}_2\text{Si}]_2$ δ [ppm]: 1.12, 0.23. $\text{Br-Si}'\text{Bu}_2\text{Me}$ δ [ppm]: 0.99, 0.30.

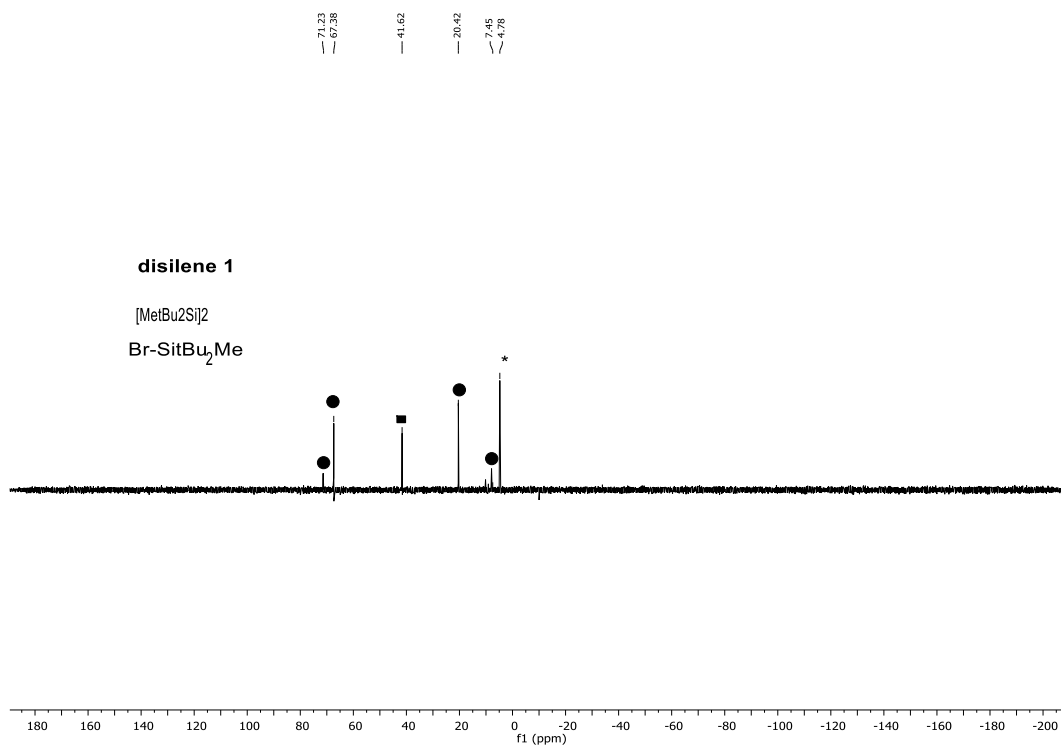
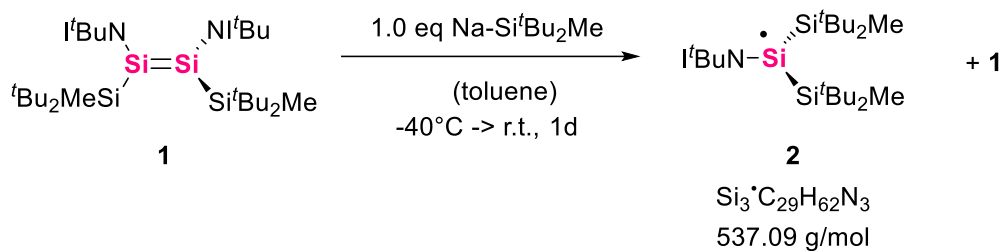


Figure 7 ^{29}Si NMR spectrum of **2**, via Pathway A. Disilene **1** δ [ppm]: 71.24, 67.37, 20.40, 7.83. Disilane $[\text{Me}'\text{Bu}_2\text{Si}]_2$ δ [ppm]: 4.77, $\text{Br-Si}'\text{Bu}_2\text{Me}$ δ [ppm]: 41.62.

1.4 Silyl Radical via Reaction Pathway B



Disilene $\text{tBuN}(\text{SiMe}_2\text{tBu})\text{Si}=\text{Si}(\text{SiMe}_2\text{tBu})\text{NtBu}$ (**1**) (42.1 mg, 55.5 μmol , 1.0 eq.) and silanide $\text{Na-SiMe}_2\text{tBu}$ (20.0 mg, 111 μmol , 1.0 eq.) were mixed, the solids cooled to -40°C , and toluene (2 mL) was added. After several minutes a white precipitate could be observed. The reaction mixture was warmed to room temperature and stirred for one day. All volatiles were removed *in vacuo*, and the residue was extracted with *n*-hexane ($3 \times 0.5 \text{ mL}$). After drying *in vacuo*, a mixture of **1** and **2** was obtained in moderate yield (38.0 mg, 70.0 μmol , 63% yield). Silyl radical **2** was verified by X-band EPR spectroscopy (Figure 6). The unusually high concentration was necessary to observe the splitting of the signals in the EPR spectrum. Using this pathway, an additional unidentified radical species could be detected. Other byproducts are imino(silyl)disilene **1** and disilane $[\text{Me}^t\text{Bu}_2\text{Si}]_2$, which were identified by ^1H and ^{29}Si NMR spectroscopy.

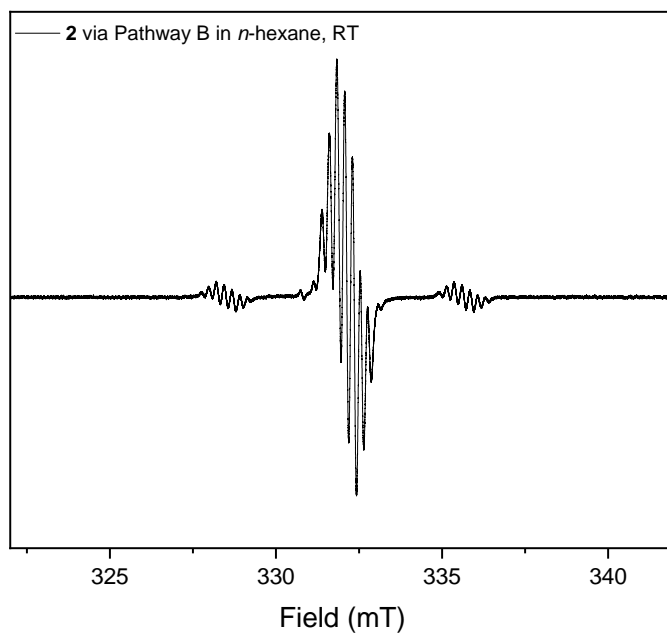


Figure 8 X-band EPR spectrum of **2**, via pathway B in *n*-hexane (2×10^{-1} M) at 286 K; (black) experimental. An additional radical species could be observed in this reaction pathway.

Table 3 Details for the EPR measurement of **2**, Pathway B.

Parameters used for the EPR measurement of 2 *	
solvent	<i>n</i> -hexane
<i>T</i> [K]	286
ν [GHz]	9.265
<i>MW</i> [mT]	0.4
<i>TC</i> [s]	0.1
<i>P</i> [mW]	5
<i>RG</i> [dB]	400
<i>CF</i> [mT]	331
<i>SW</i> [mT]	20

**T* = temperature, ν = microwave frequency, *MW* = modulation width, *TC* = time constant, *P* = microwave power, *RG* = receiver gain, *CF* = center field, *SW* = sweep width

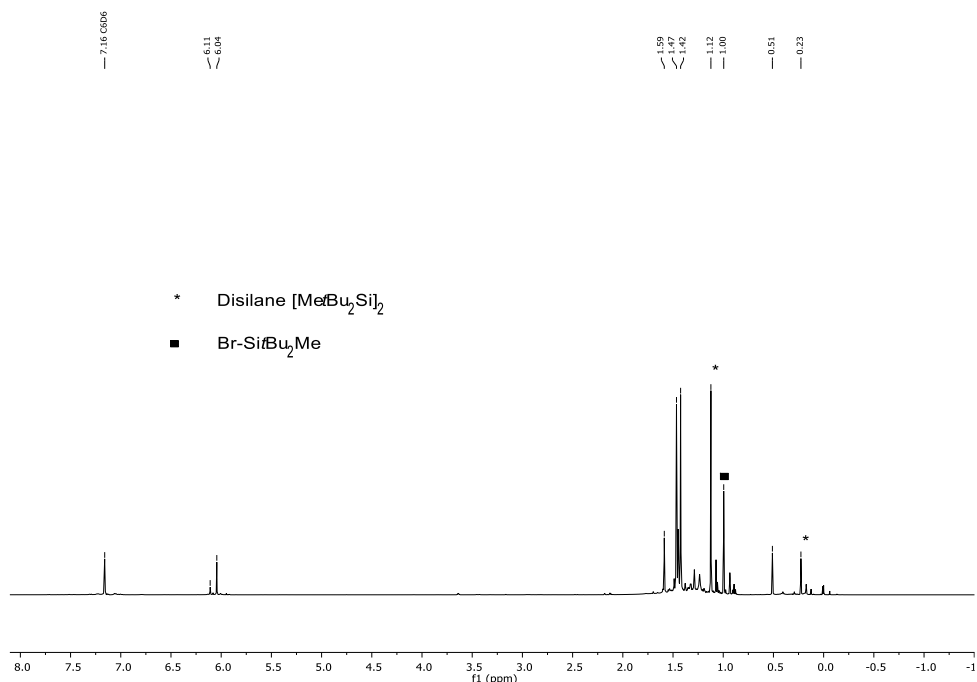


Figure 9 ¹H NMR spectrum of **2**, via Pathway B. Disilene **1** δ [ppm]: 6.11, 6.04, 1.47, 1.42, 0.51. Disilane [Me'Bu₂Si]₂ δ [ppm]: 1.12, 0.23. Br-Si'Bu₂Me δ [ppm]: 1.00.

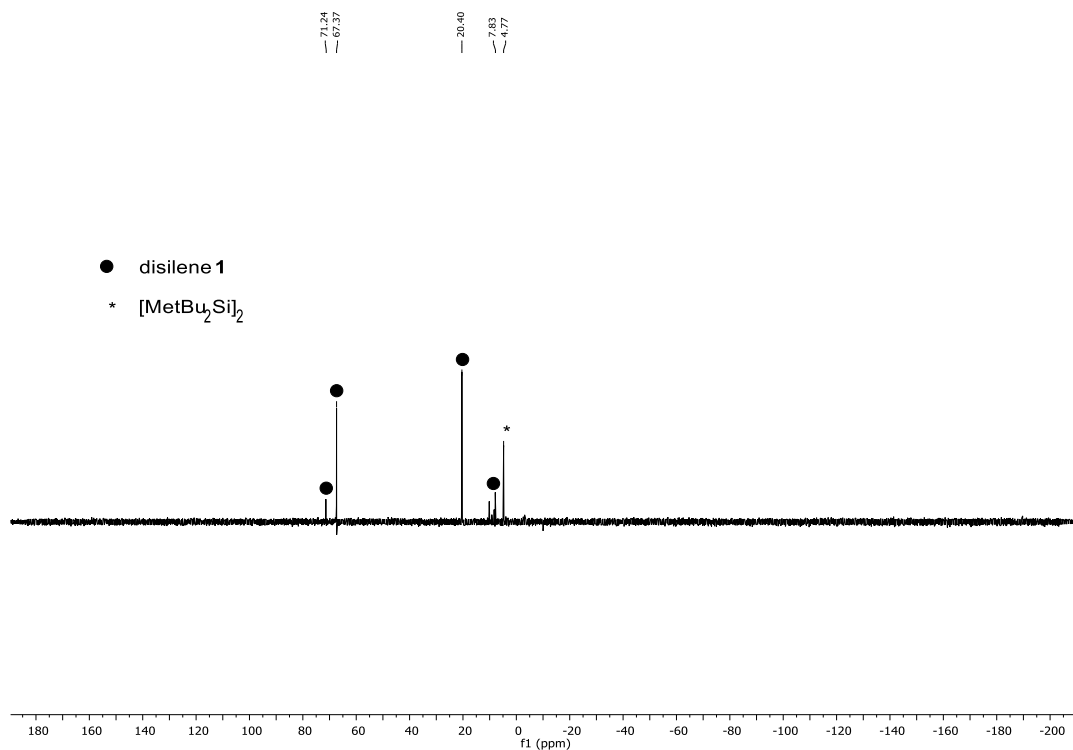


Figure 10 ²⁹Si NMR spectrum of **2**, via Pathway B. Disilene **1** δ [ppm]: 71.24, 67.37, 20.40, 7.83. Disilane [Me'Bu₂Si]₂ δ [ppm]: 4.77.

2 Single crystal X-Ray diffraction

2.1 General Information

The X-ray intensity data of **2** were collected on an X-ray single crystal diffractometer equipped with a CMOS detector (*Bruker Photon-100*), a rotating anode (*Bruker TXS*) with MoK α radiation ($\lambda = 0.71073 \text{ \AA}$) and a *Helios* mirror optic by using the *APEX III* software package.³ The measurement was performed on a single crystal coated with the perfluorinated ether *Fomblin*[®] Y. The crystal was fixed on the top of a micro sampler, transferred to the diffractometer and frozen under a stream of cold nitrogen. A matrix scan was used to determine the initial lattice parameters. Reflections were merged and corrected for Lorenz and polarization effects, scan speed, and background using *SAINTE*.⁴ Absorption corrections, including odd and even ordered spherical harmonics were performed using *SADABS*.⁴ Space group assignments were based upon systematic absences, E statistics, and successful refinement of the structures. The structure was solved by direct methods with the aid of successive difference Fourier maps, and was refined against all data using the *APEX III* software in conjunction with *SHELXL-2014*⁵ and *SHELXLE*.⁶ For refinement of **2**, a twin refinement model with the matrix [-1 0 0 0 -1 0 -0.419 -0.716 1] and BASF 0.01312 was used. A minor pyramidal disorder of the central Si1 atom was addressed with a disorder occupancy of 6.38% (Si1D). All H atoms (except Si–H) were placed in calculated positions and refined using a riding model, with methylene and aromatic C–H distances of 0.99 and 0.95 Å, respectively, and $U_{\text{iso}}(\text{H}) = 1.2 \cdot U_{\text{eq}}(\text{C})$. H atoms bound to Si atoms could be located in the difference Fourier maps and were allowed to refine freely. Full-matrix least-squares refinements were carried out by minimizing $\Delta w(F_o^2 - F_c^2)^4$ with *SHELXL-97* weighting scheme.⁵ Neutral atom scattering factors for all atoms and anomalous dispersion corrections for the non-hydrogen atoms were taken from International Tables for Crystallography.⁷ The images of the crystal structures were generated by *Mercury*.⁸ The CCDC number 2352376 contains the supplementary crystallographic data for the structures. The data can be obtained free of charge from the Cambridge Crystallographic Data Centre via <https://www.ccdc.cam.ac.uk/structures/>.

2.2 SC-XRD Structure

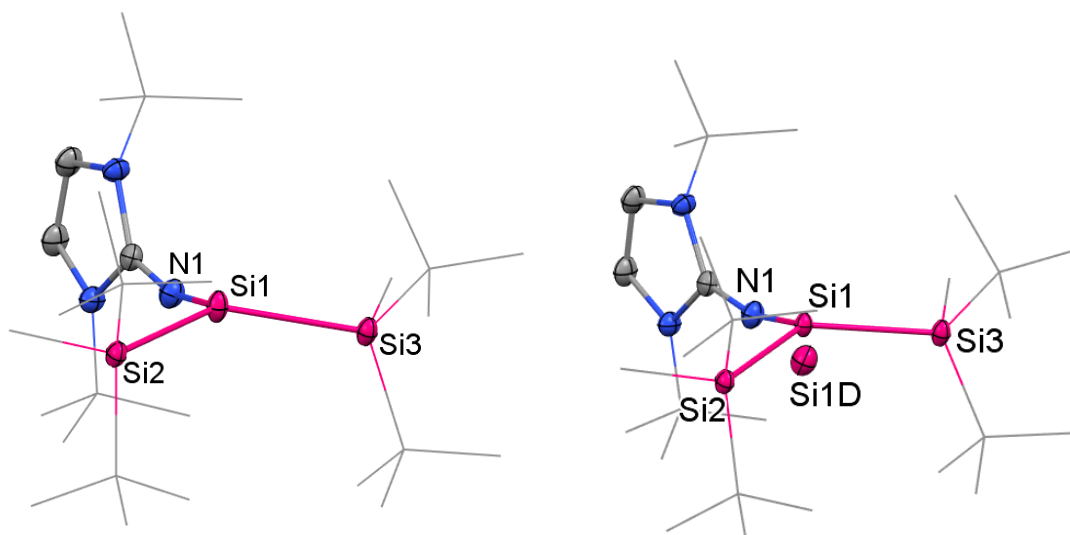


Figure 11 SC-XRD structure of neutral silyl radical **2**, with thermal ellipsoids drawn at the 50% probability level. Hydrogen atoms are omitted for clarity, ^tBu- and Me-groups are simplified as wireframes. Central Si1 is in a pyramidal disorder (Si1D) with an occupation of 6.38%. Twin refinement was conducted with the matrix $-1\ 0\ 0\ 0\ -1\ 0\ -0.419\ -0.716\ 1$ and BASF 0.01312. Selected bond lengths [Å] and angles [°]: Si1–Si2 2.3843(7), Si1–Si3 2.3790(8), Si1–N1 1.676(2), N1–C1 1.280(3), Si2–Si1–Si3 132.98(3), Si3–Si1–N1 108.91(7), N1–Si1–Si2 111.62(7). Sum of bond angles: 353.51° (Si1), 352.42° (Si1D).

2.3 Crystal Data and Structural Refinement Parameters

	2
CCDC Number	2352376
Crystal Data	
Chemical formula	$C_{29}H_{62}N_3Si_3$
M_r	537.09
Crystal system, space group	Triclinic, P^1
Temperature (K)	100
a, b, c (Å)	11.5884 (10), 17.2210 (16), 18.5360 (17)
α, β, γ (°)	69.558 (3), 80.011 (3), 82.655 (3)
V (Å ³)	3404.6 (5)
Z	4
$F(000)$	1196
Radiation type	Mo $K\alpha$
No. of reflections for cell measurement	9951
q range (°) for cell measurement	2.28 – 28.48
μ (mm ⁻¹)	0.16
Crystal shape	Fragment
Colour	Clear red-orange
Crystal size (mm)	0.39 × 0.33 × 0.32
Data Collection	
Diffractometer	APEX II CCD
Radiation source	fine-focus sealed tube
Detector resolution (p mm ⁻¹)	16
Scan method	phi- and ω -rotation scans
Absorption correction	Multi-scan
T_{\min}, T_{\max}	0.717, 0.746
No. of measured, independent and observed [$I > 2\sigma(I)$] reflections	119802, 12891, 11639
R_{int}	0.028
q values (°)	$q_{\max} = 25.68, q_{\min} = 1.18$
$(\sin \theta/\lambda)_{\max}$ (Å ⁻¹)	0.610
Range of h, k, l	$h = -14 \rightarrow 14, k = -20 \rightarrow 20, l = -22 \rightarrow 22$
Refinement	
Refinement on	F^2
$R[F^2 > 2\sigma(F^2)], wR(F^2), S$	0.040, 0.103, 1.12
No. of reflections	12891
No. of parameters	672
H-atom treatment	H-atom parameters constrained
Weighting scheme	$w = 1/[\sigma^2(F_o^2) + (0.0262P)^2 + 4.1668P]$ where $P = (F_o^2 + 2F_c^2)/3$

$\Delta\rho_{\max}, \Delta\rho_{\min} (e \text{ \AA}^{-3})$	1.12, -58
---	-----------

3 Computational Details

3.1 General Information

The quantum chemical calculations were performed using ORCA 5.0.4 software.⁹ Geometry optimizations were carried using the r^2 SCAN-3c composite method, utilizing the regularized and restored SCAN functional,^{10,11} geometrical counterpoise correction gCP,¹² the atom-pairwise dispersion correction based on tight binding partial charges (D4),^{13–15} the def2-mTZVPP basis set and def2-mTZVPP/J auxiliary basis set.¹⁶ The optimized geometries were verified as minima by analytical frequency calculations. The isotropic g-tensor and the isotropic hyperfine coupling constants (hffcc) of the r^2 SCAN-3c were calculated at the B3LYP^{17–20}/IGLO-III²¹ level of theory with def2/J²² auxiliary basis set. The NBO analysis was done using the NBO7 software.²³ The EPR spectrum using the B3LYP/IGLO-III// r^2 SCAN-3c obtained EPR parameters was simulated using EasySpin 6.0.0 software.² For the fitting of the experimental spectrum we used an initial system, which included the three Si atoms, i.e. the α -silicon atom and the two β -silicon atoms, and the three nitrogen atoms, i.e. the β -nitrogen atom and the two nitrogen atoms of the NHC moiety. For the definition of the initial system, we used the hffcs for these six atoms that we obtained from the DFT calculations. The system was generated using the “garlic” function. In the fitting of the system to the experimental spectrum we allowed for the variation for the six hffcs, as well the line width and g-strain.

3.2 Cartesian coordinates and energies of the optimized geometries at the r^2 SCAN-3c level

Calculated energies and coordinates of 2	C	11.777026	2.588339	7.247088
	C	6.974868	4.669439	4.524710
Electronic energy	...	-2174.78375708 Eh		
Total Enthalpy	...	-2173.87066356 Eh		
Final Gibbs free energy	...	-2173.99046996 Eh		
CARTESIAN COORDINATES (ANGSTROEM)				
Si	10.228133	5.312224	3.981564	
Si	8.027746	6.230375	4.275969	
Si	12.460420	6.185003	4.014291	
N	10.290898	3.744048	4.637783	
N	9.960372	1.549843	3.607580	
N	9.993831	1.693030	5.822471	
C	10.090553	2.477673	4.658652	
C	9.795157	0.273180	4.134845	
C	9.826900	0.359798	5.476302	
C	10.071626	1.841932	2.153746	
C	11.411958	2.527192	1.864830	
C	10.019695	0.532326	1.360114	
C	8.897316	2.722058	1.724718	
C	10.302616	2.171119	7.195414	
C	10.066139	1.039970	8.199818	
C	9.382230	3.339444	7.556050	
	C	11.777026	2.588339	7.247088
	C	6.974868	4.669439	4.524710
	C	7.662579	7.354035	5.827717
	C	8.378648	6.768331	7.055000
	C	6.156288	7.359844	6.155449
	C	8.122629	8.805205	5.624062
	C	7.485630	7.071627	2.609241
	C	6.080058	7.687579	2.694862
	C	8.487293	8.154260	2.183851
	C	7.461214	6.008394	1.498297
	C	13.543662	4.623953	3.970532
	C	12.918151	7.127440	5.648627
	C	12.787699	6.113293	6.797316
	C	11.959612	8.289251	5.934251
	C	14.357831	7.664029	5.633273
	C	12.881436	7.172532	2.394988
	C	12.402640	8.630279	2.458464
	C	14.401901	7.169492	2.144271
	C	12.221266	6.479187	1.190963
	H	9.643064	-0.598923	3.524678
	H	9.705099	-0.424750	6.201949
	H	11.525366	2.664747	0.784469
	H	12.242636	1.913920	2.229823

H	11.463630	3.507561	2.340191
H	10.114501	0.779733	0.299344
H	9.067907	0.007373	1.491193
H	10.843999	-0.139087	1.622125
H	8.971319	2.955542	0.657263
H	8.904371	3.664781	2.274709
H	7.945935	2.209874	1.905295
H	9.032912	0.677798	8.168266
H	10.250785	1.435374	9.202553
H	10.749467	0.198553	8.047481
H	9.512472	4.161240	6.854257
H	9.615517	3.694681	8.565308
H	8.334363	3.019609	7.534902
H	12.422665	1.729125	7.034892
H	12.025924	2.976357	8.240506
H	11.975144	3.369462	6.512713
H	5.908950	4.886273	4.386193
H	7.111090	4.278957	5.538928
H	7.252436	3.870034	3.832997
H	9.459466	6.678220	6.907335
H	7.992129	5.774511	7.302497
H	8.209511	7.413405	7.929805
H	5.546325	7.768489	5.345830
H	5.980087	7.982155	7.045438
H	5.786285	6.354622	6.382741
H	9.166596	8.872192	5.302049
H	8.032053	9.361356	6.568535
H	7.509805	9.325221	4.881130
H	5.779678	8.053039	1.701844
H	6.037252	8.541240	3.377430
H	5.327824	6.956414	3.013568
H	9.489225	7.727288	2.070261
H	8.549639	8.980694	2.897964
H	8.198594	8.577215	1.210237
H	7.123616	6.467426	0.557391
H	6.779946	5.180655	1.726722
H	8.459567	5.593177	1.326890
H	13.634415	4.235814	2.951327
H	13.120577	3.826010	4.587607
H	14.555332	4.842680	4.332051
H	11.780124	5.681456	6.836834
H	12.978003	6.609796	7.760175
H	13.504178	5.290214	6.699869
H	12.013847	9.075826	5.176026
H	12.196878	8.746805	6.906123
H	10.925951	7.936799	5.978965
H	15.091660	6.888472	5.385472
H	14.617740	8.054596	6.628378
H	14.479025	8.487412	4.921859
H	12.530393	9.113502	1.478620
H	12.980093	9.211464	3.184892
H	11.344570	8.712010	2.729126
H	14.791434	6.154228	2.016314
H	14.964060	7.645264	2.952555
H	14.621721	7.723723	1.219804
H	12.494092	7.004751	0.263856
H	11.129411	6.463789	1.267933
H	12.553428	5.439012	1.090108

4 References

- 1 R. Holzner, A. Porzelt, U. S. Karaca, F. Kiefer, P. Frisch, D. Wendel, M. C. Holthausen and S. Inoue, *Dalton Trans.*, 2021, **50**, 8785–8793.
- 2 S. Stoll and A. Schweiger, EasySpin, *J. Magn. Reson.*, 2006, **178**, 42–55.
- 3 *APEX 4*, Bruker AXS Inc.: Madison, Wisconsin, USA, Madison, Wisconsin, USA, 2020.
- 4 G.M. Sheldrick, *SADABS*, Bruker AXS Inc.: Madison, Wisconsin, USA, Madison, Wisconsin, USA, 2008.
- 5 G. M. Sheldrick, *Acta Cryst. Section C, Struct. Chem.*, 2015, **71**, 3–8.
- 6 C. B. Hübschle, G. M. Sheldrick and B. Dittrich, *J. Appl. Cryst.*, 2011, **44**, 1281–1284.
- 7 A. J. C. Wilson and V. Geist, *Cryst. Res. Technol.*, 1993, **28**, 110.
- 8 C. F. Macrae, I. Sovago, S. J. Cottrell, P. T. A. Galek, P. McCabe, E. Pidcock, M. Platings, G. P. Shields, J. S. Stevens, M. Towler and P. A. Wood, *J. Appl. Cryst.*, 2020, **53**, 226–235.
- 9 F. Neese, Software update: The ORCA program system—Version 5.0, *WIREs Comput. Mol. Sci.*, 2022, **12**.
- 10 J. W. Furness, A. D. Kaplan, J. Ning, J. P. Perdew and J. Sun, *J Phys. Chem. Lett.*, 2020, **11**, 9248.
- 11 J. W. Furness, A. D. Kaplan, J. Ning, J. P. Perdew and J. Sun, *J Phys. Chem. Lett.*, 2020, **11**, 8208–8215.
- 12 H. Kruse and S. Grimme, *J. Chem. Phys.*, 2012, **136**, 154101.
- 13 E. Caldeweyher, C. Bannwarth and S. Grimme, *J. Chem. Phys.*, 2017, **147**, 34112.
- 14 E. Caldeweyher, S. Ehlert, A. Hansen, H. Neugebauer, S. Spicher, C. Bannwarth and S. Grimme, *J. Chem. Phys.*, 2019, **150**, 154122.
- 15 E. Caldeweyher, J.-M. Mewes, S. Ehlert and S. Grimme, *Phys. Chem. Chem. Phys.*, 2020, **22**, 8499–8512.
- 16 S. Grimme, A. Hansen, S. Ehlert and J.-M. Mewes, *J. Chem. Phys.*, 2021, **154**, 64103.
- 17 P. J. Stephens, F. J. Devlin, C. F. Chabalowski and M. J. Frisch, *J. Phys. Chem.*, 1994, **98**, 11623–11627.
- 18 S. H. Vosko, L. Wilk and M. Nusair, *Can. J. Phys.*, 1980, **58**, 1200–1211.
- 19 C. Lee, W. Yang and R. G. Parr, *Phys. Rev. B*, 1988, **37**, 785.
- 20 A. D. Becke, *J. Chem. Phys.*, 1992, **96**, 2155–2160.
- 21 W. Kutzelnigg, U. Fleischer and M. Schindler, *NMR basic principles and progress*, 1990, **23**, 165–262.
- 22 F. Weigend, *Phys. Chem. Chem. Phys.*, 2006, **8**, 1057–1065.

23 E. D. Glendening, J. K. Badenhop, A. E. Reed, J. E. Carpenter, J. A. Bohmann, C. M. Morales, P. Karafiloglou, C. R. Landis and F. Weinhold, *NBO 7.0, Theoretical Chemistry Institute, University of Wisconsin, Madison, 2018.*